NATIONAL AIR INTELLIGENCE CENTER
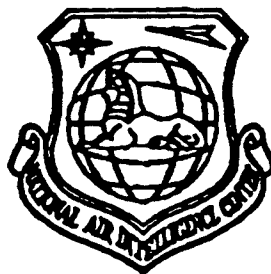
MODEL JC-1 LASER SYSTEM FOR MONITORING
ATMOSPHERIC POLLUTION
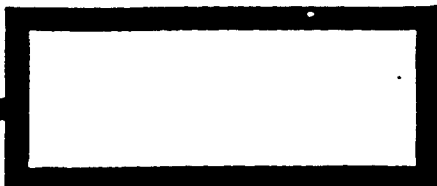
by

Lu Xinqi, Ji Guangde, et al.

19970206 014

HUMAN TRANSLATION

NAIC-ID(RS)T-0572-96   29 January 1997

MICROFICHE NR:

MODEL JC-1 LASER SYSTEM FOR MONITORING ATMOSPHERIC POLLUTION

By: Lu Xinqi, Ji Guangde, et al.

English pages: 12

Source: Applied Laser Technology; pp. 29-32

Country of origin: China
Translated by: Leo Kanner Associates
                F33657-88-D-2188
Requester: NAIC/TATD/Bruce Armstrong
Approved for public release: distribution unlimited.

GRAPHICS DISCLAIMER

All figures, graphics, tables, equations, etc. merged into this
translation were extracted from the best quality copy available.

MODEL JC-1 LASER SYSTEM FOR MONITORING
ATMOSPHERIC POLLUTION

Lu Xinqi, Ji Guangde, He Renping,
Wang Zhenbo, Fan Siliang, and Luo Xiougyan

Anhui Institute of Optics and
Fine Mechanics
Chinese Academy of Sciences

Chen Huaiyu and Liu Wei
Anhui Environmental Monitoring Station

Abstract: This paper introduces the basic principle
and structure of the model JC-1 laser system for
monitoring atmospheric pollution that has been developed.
At the same time, we also describe the experimental results
of monitoring the pollutant ethylene in the field and
the count methods of monitoring parameters for this system.

With the advances in laser and spectrum technology, a number
of advanced laser monitoring systems for atmosphere pollution
have appeared in the past several years. Featuring high
sensitivity and high resolution, a system of this kind can carry
out automatic, continuous and real-time non-interference
monitoring over pollution sources over a large area and at high
altitudes.

Basically, with a beam-selection CW CO_2 laser as the light
source, we developed a differential absorption mode atmospheric

pollution laser monitoring system, in which a phase locking technique and single board computer are used for data processing as shown in Fig. 1.

To meet the requirements from the petrochemical industry, in 1985, in collaboration with the Anhui Environmental Monitoring Station, a long-term outdoor quantitative test and investigation of ethylene was conducted by using this system at our institute. The test results suggested that this sample system has stable performance, and that all its technical indicators reached the application standard.

At an optical distance of 600m, the minimum monitoring concentration value of this system was 2.47ppm. In addition, it can also be used to monitor vinyl chloride and ozone. What is more, by changing the laser beam source, this system can also realize the on-site real-time monitoring of NO^X, SO_2 and CO.

Design Principle

The attenuation of the laser beam propagating through the uniform atmosphere is as follows:

$$P_R(\lambda) = P_0(\lambda)\exp[-K(\lambda)\cdot L] \tag{1}$$

where $P_0(\lambda)$ is laser transmission power, $P_R(\lambda)$ is the power received after propagating over a distance L, $K(\lambda)$ is the overall extinction coefficient at a laser wavelength λ. Under actual conditions, Eq. (1) becomes:

$$\frac{P_R(\lambda)}{P_0(\lambda)} = T\cdot S(t)\exp\left[-L\left(\sum_{i=1}^{N} K_{ai}\cdot C_i\right)\right] \cdot \exp(-Ks_i L) \tag{2}$$

where T is the optical-system efficiency of the monitoring system; S(t) is the variation ratio of the laser power excited by the atmospheric turbulence effect versus time; N is the number of various gases; K_{ai} is the absorption coefficient of the absorbing

2

gas; C_i is the gas concentration; K_{ai} is the overall extinction coefficient resulting from Rayleigh scattering and Mie scattering of atmospheric molecules, aerosol and particles.

Obviously, the absorption of components other than the measured pollutant gases, the power attenuation caused by aerosol and particle scattering, as well as the fluctuation of laser power resulting from the turbulence effect, can all give rise to background interference and can severely affect the monitoring accuracy. Thus, the foregoing factors must be eliminated during the monitoring of certain atmosphere pollutant at a given wavelength. Nevertheless, this seems to be fairly complicated and even is considered to be impossible.
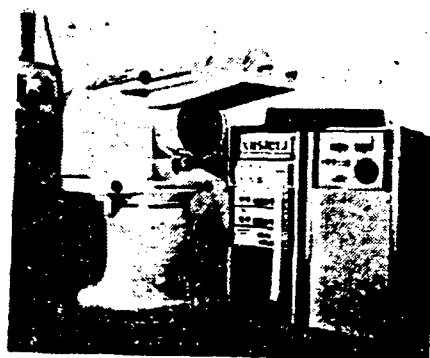

Fig. 1. Photograph of JC-1 laser system for monitoring atmospheric pollution

When we selected two mutually closed wavelengths λ_1 and λ_2 in conducting the measurements, an equation similar to Eq. (2) can be obtained, respectively, for both the two laser wavelengths, and then by dividing these two equations, the following can be derived:

$$\frac{P_R(\lambda_1) \cdot P_0(\lambda_2)}{P_0(\lambda_1) \cdot P_R(\lambda_2)} = \frac{T_1 \cdot S(t)}{T_2 \cdot S(t+\tau)} \exp\left\{ -L \sum_{i=1}^{N} [K_{ai}(\lambda_1) - K_{ai}(\lambda_2)] \cdot C_i \right\} \cdot \exp\left\{ -L[K_e(\lambda_1) - K_e(\lambda_2)] \right\}$$

(3)

3

Since the Mie scattering of aerosol and particles as well as the Rayleigh scattering of middle infrared atmospheric molecules can be regarded as a diffuse variable function of wavelength, the difference between the two selected wavelengths is only several percent of a micrometer, $K_s(\lambda_1)-K_s(\lambda_2)$. However, if the laser device and the optical system are well designed, $T_1=T_2$ can be achieved. Again, if the transmission interval τ between the two laser devices is fairly small($\approx$1ms), and coaxial transmission of the laser beam is adjusted, then $S(t)\approx S(t+\tau)$ can be obtained; that is because the strong frequency distribution area of the turbulence is below 100cycles.

Prior to the design of the overall monitoring system, a large number of indoor simulation experiments were done, in which the absorption coefficients of every relevant absorbing component to various laser spectral lines were comprehensively analyzed. Based on the analysis, two extremely closed wavelengths were selected to form a pair of monitoring lines, at which a certain pollutant element to be measured was allowed to reach its maximum absorption difference, while the other absorbing elements was allowed to have the minimum absorption difference. At this point, Eq. (3) can be simplified as follows:

$$\frac{P_R(\lambda_1)\cdot P_0(\lambda_2)}{P_0(\lambda_1)\cdot P_R(\lambda_2)}=\exp(-L\cdot\Delta K_\lambda\cdot C) \tag{4}$$

from which, the average pollution concentration C at the interval to be measured can be derived.

If in the monitoring environment there are a variety of gases that show a considerable absorption difference and concentration, then a multi-wavelength measurement must be done, and many pairs of monitoring lines must be selected, in which each equation takes on a form similar to Eq. (4). Then, through the solution of the coupled equation, the concentration of the pollutant to be measured can be obtained.

Overall System Structure and Features

This system was in fact a single-ended system with a corner reflector as a cooperative target, with its block diagram shown in Fig. 2. Structurally, the overall system was composed of three parts: laser source, optics system, and signal processing system, of which the optical system was placed in the azimuth and pitch adjustable platform consisting of a worm wheel and worm screw driving mechanism.

In order to effectively overcome the turbulence effect, we applied two laser devices with different working wavelengths, thereby affording a simultaneous and coaxial transmission.

The cavity length of the two developed CW CO_2 beam-selection laser devices was 1000mm; the original concave plane metal raster was taken as a disperse component with the number of graduation lines as 100lines/mm; first level oscillation; first level output; strong line output power 8.4W; single transverse mode output; the beam divergent angle 1.69mrad, and the instability of output power being less than 5%.

When the ethylene was detected, these two laser devices were tuned, respectively, to the strong absorption line of the ethylene (P_{14} in 00^01-10^00 zone) and the weak absorption line of the ethylene (P_{20} in 00^01-10^00 zone). Also, these two laser beams, respectively, were modulated by a chopper as 18.45 and 30.48cycles per second, and at the same time were split, respectively, into two beams. Thus, a small amount of energy in either of the laser devices was received by detectors D_1 and D_2 as a way of monitoring the stability of the output power.

Meanwhile, the other two laser beams with the majority of energy, respectively, were adjusted to be coaxial with the collimation-oriented He-Ne laser. Then, through a rotary mirror,

these three coaxial beams passed through a reflecting telescope
(the bore of the main mirror was OD300) with a beam expansion
ratio 1:30 to be expanded before being transmitted. At this
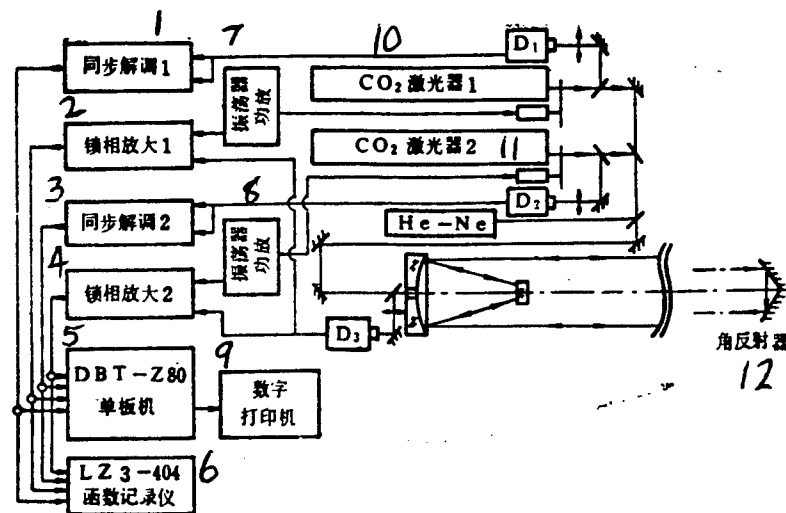point, the divergent angle was only 0.053mrad.

Fig. 2 JC-1 laser system for monitoring
atmospheric pollution
KEY: 1. synchronous demodulation 1
      2. phase locking amplification 1
      3. synchronous demodulation 2
      4. phase locking amplification 2
      5. single board computer
      6. function logging Instrument
      7. oscillator power amplification
      8. oscillator power amplification
      9. digital Printer
      10. CO_2 laser device 1
      11. CO_2 laser device 2
      12. corner reflector

These two coaxially transmitted laser beams, after
travelling a distance L/2, were sent back along the original
optical path by the corner reflector with side length 140mm, and
then were focused on the detector D_3. The signal received by the
D_3 was $P_r(\lambda_1) + P_r(\lambda_2)$. The amplified $P_0(\lambda_1)$ and $P_0(\lambda_2)$ were sent
to the dual-channel synchronous demodulator, through which two

corresponding direct current values were derived.

Through the separation of the amplified $P_r(\lambda_1) + P_r(\lambda_2)$ by two phase locking amplifiers, another two direct current values corresponding to the $P_r(a_1)$ and $P_r(a_2)$ were obtained. These four direct current values were, in turn, converted to four corresponding digital values through a 12-bit data collector, and were then fed into a DBJ-Z80 single-board computer to undergo a multiple averaging process before going through functional operation, and were logged and printed. Finally, the average concentration (or the integrated concentration value) of the measured pollutant was derived, while the x-y function logging device was used for monitoring.

This system has following features:

(1) For the drive chain of the master unit, a larger drive ratio (i=3000) was selected to enhance the center-aligned capability of the master unit over the target so that the system can accurately aim at the target even in the daytime. Among other things, this system was convenient to operate with two pairs of worm wheel and worm screw applied in the azimuth and pitch adjustment and it had a strong self-locking property. A chassis base was installed in the laser device and optical system for reinforcement purpose; a one-time adjustment locking system was applied in each of the optical path adjustment frames, among which, the major mirror frame was made of cast iron to ensure a stable and reliable operation of the optical path system.

(2) Multilevel rasters were fixed on the laser discharge tubes, and the beam was chosen through concave raster to ensure an output of the TEM_{00} mode. The raster adjustment frame was controlled with a rotating axis tangent rotary platform and a differential micrometer so that it could be adjusted conveniently and reliably. Moreover, the raster frame was connected with the tube through a quartz pipe as a transition ensuring the integrity

7

of the components. Therefore, under the premise of stable operating conditions, the structure can be simplified and costs can be reduced.

(3) A reflecting telescope with a beam expansion ratio 1:30 and an effective bore OD300 was used for both reception and transmission. At the same time, the subsidiary mirror can be tuned along the optical axis direction so that the transmitting beam can be converged properly through adjustment to allow all-wave reception and improvement of the test accuracy.

(4) A single-board computer was used in data processing. In order to improve the low computing capability of this computer, an arithmetic database was inserted in the board of this computer to strengthen its computing performance. Furthermore, a VOESA1871 PD mini-printer was designed for reducing the volume and cost of the computer. To further avoid the turbulence effect, Z80 machine language coding was selected for rapid collection of four path signals. Additionally, the printing interval can be chosen between from 2s to 9999s, depending on user requirements.

(5) Two special DS-1 low temperature drift phase locking amplifiers were developed based on the overall requirements. With these amplifiers, auto-tracking of both return wave signals and reference signals can be achieved through internal synchronous operation, which not only enhanced the stability of the system, but also simplified the circuit structure.

Field Test Result and Computing Method

According to the monitoring standards and computational rules regulated by the National Environment Protection Department in regard to environmental monitoring equipment, an item-by-item test involving various technical indicators was performed on

these two systems, with the results shown in Table 1 and Fig. 1.

The major technical indicators derived from the test on
these two systems are as follows:
(1) minimum measurement level 2.47ppm·m; (2) measurement
concentration range, 2.47~212.4ppm·m; (3) measurement
correctness, i.e., the maximum relative error 3.8%;
(4) measurement accuracy: the maximum variation coefficient 3.5%;
(5) response time less than 10s.

TABLE 1 表1 实测结果 /

注入次数 2	1	2	3	4	5	6
C_2H_4(ml)	0	1	3	8	13	15
折合积分浓度(ppm·m) 3	0	14.16	42.49	113.3	184.1	212.4
响应值 4	80.7	124.5	225.7	464.9	720.0	816.4
标准偏差 5	2.86	3.39	4.39	12.2	5.82	5.67
测定结果(ppm·m) 6		13.6	42.7	111.5	184.9	212.6
相对误差% 7		−3.8	−0.28	−1.5	+0.43	+0.09
变异系数% 8	3.5	2.7	1.9	2.6	0.8	0.7

KEY: 1. actual measurement result
     2. times of injection
     3. converted integration concentration
        (ppm·m)
     4. response value
     5. standard deviation
     6. measured result (ppm·m)
     7. relative error %
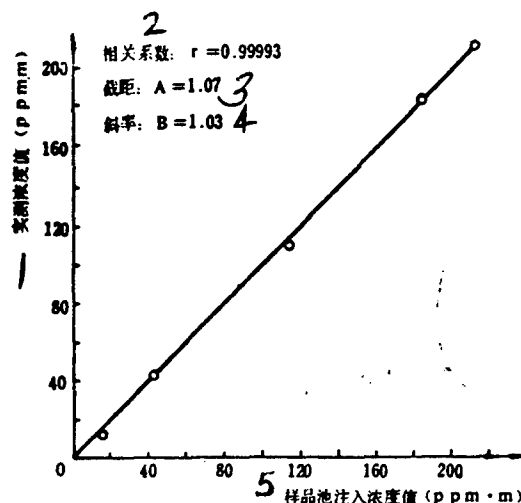   8. variation coefficient %

Fig 3. Linear correlation between injection
concentration and actual measurements
KEY: 1. measured concentration value (ppm.m)
     2. correlation coefficient r=0.99993
     3. distance A=1.07
     4. slope B=1.03
     5. injection concentration value (ppm·m)
     in the sample pool

Testing and Computational Method

    (1) Determination of minimum measurement

    The corner reflector was placed at a distance of 300m, and
an empty sample pool was inserted in the optical path. When the
device was brought to a stable condition, the test results were
continuously printed out, of which over 20 consecutive measured
values were selected for computing their standard difference.
And then a minimum detected value (unit ppm·m) was obtained
according to $D=3S_b/B$, where S_b is the standard difference of the
response value; the computational formula is

$$S_b = \sqrt{\sum_{i=1}^{n} (x_i - \bar{x}_i)^2/(n-1)}$$; B is the slope of the regression formula
of the measured value vs standard sample concentration value.

(2) Test for monitoring concentration range. The ethylene standard gas was continuously injected into the empty sample pool, and its response values, respectively, were measured. Taking the response value as the longitudinal axis and the injection value as the transverse axis, the function graphic line was plotted using the tracing point method, and then the breakpoint of the curve was determined. The measurement range of this system extended from the minimum detected value to the X value corresponding to the breakpoint.

(3) Test of correctness and accuracy. The ethylene standard gas of 0, 1, 3, 8, 13 and 15mL, respectively, were injected into the sample pool, and more than 20 data were, respectively, measured; the standard difference S_i and average value $\bar{x}_i$ were computed, respectively. The measurement accuracy was $(\bar{x}_i - x_{si})/x_{si}$, where $\bar{x}_{si}$ was the injected standard gas value, while $S_i/\bar{x}_i$ was the average value of the measured value.

(4) Test of response time. The empty pool was inserted in the optical path, and after the instrument reached a stable condition, a fixed quantity of ethylene was injected; the results were continuously printed out. When the time needed from injecting the standard gas to printing the result was equivalent to 90% of the stable value, this time was set as the response time of the device (the response time measured with this method was in fact longer than the actual response time of the instrument because it included the sample dispersion time).

(5) Experiment with the correction curve and analysis of linear regression.
Following continuous injection of standard ethylene into the sample pool and measurement of respective response values, the regression equation of the test result was derived by using the minimum square method as follows: $\hat{y} = 77.1 + 3.47\, x$

$$v = \frac{\Sigma x \cdot y - \Sigma x \cdot \Sigma y / n}{\sqrt{[\Sigma x^2 - (\Sigma x)^2/n] \cdot [\Sigma y^2 - (\Sigma y^2)/n]}}$$

The value $v = 0.99993$ was derived based on the test result.

Participating in this project were Zhou Younan, Wang Ruxiang, Gao Minguang, Cai jinfeng, Yan Jianhua, Gao Yijiao, Liu Mujin, and Cheng Yuzheng. Special thanks are due Song Zhenfang, Wu Jihua, and Tan Kun from the Anhui Environmental Monitoring Central Station and the Anhui Institute of Optics and Fine Mechanics for their vigorous support.

This paper was received on May 2, 1986.